Study for Emittance Measurements in a High-Current Multibeamlet Beam*)

Emanuele SARTORI[1,2], Matteo ZAUPA[1], Gianluigi SERIANNI[1] and Roberto PASQUALOTTO[1]

[1] *Consorzio RFX (CNR,ENEA,INFN,Università di Padova,Acciaierie Venete SpA), C. Stati Uniti 4, 35127 Padova, Italy*

[2] *Universita' degli Studi di Padova, Department of Management and Engineering, Padua, Italy*

(Received 28 December 2017 / Accepted 24 May 2018)

SPIDER is the prototype beam source of the ITER Heating Neutral Beam injector. A movable diagnostic calorimeter will be used as a direct mean to obtain the beam footprint in short-pulses, while a fixed beam-dump is installed for steady-state operation. For the comparison between experiment and numerical simulations of ion beam extraction, measuring the beam emittance is extremely useful, being the most complete characterization for a particle beam. We discuss in this paper two proposals for beam-emittance measurements in SPIDER: at high beam energies, a fixed electric-sweep scanner is proposed for integration in the water-cooled beam-dump; at relatively low beam energies, a movable emittance scanner is proposed for the installation on the movable diagnostic calorimeter. The synthetic signals of the scanner are calculated considering the multibeamlet setup. The constraints given by the integration in high heat load components and the thermal design are discussed. The fixed ESS can be used to reconstruct the beam divergence, even if it detects only a limited section of the beamlet emittance, if identical single-beamlet optics is assumed. The movable emittance scanner is easy to integrate in the present design, and allows a full characterization of the single beamlet optics.

Keywords: ITER Neutral Beam Injector, beam emittance, multibeamlet, negative hydrogen ion beam, SPIDER

DOI: 10.1585/pfr.13.3405092

1. Introduction

SPIDER [1] is the high-current, multi-beamlet, prototype beam source of the ITER Heating Neutral Beam (HNB) [2] injector. The nominal beam parameters are 56A H^- beam (40 D^-), accelerated at an energy up to 110 keV, arranged in 1280 beamlets. A heat flux up to 5 MW/m^2 is expected at the beam dump at full power. The purpose of SPIDER is to optimize the ion source for the use in the HNB, by demonstrating beam uniformity and reasonably good single-beamlet optics: to this purpose, measuring the beam properties is essential. A movable diagnostic calorimeter will be used in short pulses as a direct means to obtain the overall beam footprint [3]; for long, high-power pulses, a rough characterization of the beam profile will be obtained from a water-cooled beam dump with embedded thermocouples [4], whereas the beam divergence will be obtained by beam emission spectroscopy [5]. However, to provide the complete beam characterization necessary for direct comparison with numerical codes, measuring the beam emittance is necessary.

In this work, we discuss two proposals for beam emittance measurement. A fixed electric-sweep scanner [6] (ESS) is proposed for integration in the beam dump: with a simple setup, the proposed ESS gives a partial measurement of the multi-beamlet emittance. The beamlet divergence can be inferred from this measurement, while it provides a direct estimate of the beam ion temperature and halo component. A movable emittance scanner (Allison scanner) is proposed for the installation on the movable diagnostic calorimeter STRIKE: this movable solution allows measuring single-beamlet emittance, but its use is limited to short pulses, or relatively low beam power.

2. Beam Description in Phase Space

The synthetic signals of the emittance scanners is constructed from the single-beamlet Twiss parameters [7], which at the grounded grid $z = 0$ can be estimated, with E_b beam energy and ε single-beamlet emittance, as follows

$$\begin{cases} \beta(0) = r_b^2/\varepsilon \\ \gamma(0) = \delta_b^2/\varepsilon \\ \alpha(0) = p\sqrt{\gamma(0)\beta(0) - 1}, \end{cases} \tag{1}$$

assuming both beamlet current density and velocity distribution have Gaussian distribution, with standard deviation r_b and δ_b respectively. We also assumed the existence of a temperature T_{H^-} for the beam particles. The drift matrix in the emittance space is

$$\begin{pmatrix} x(L) \\ x'(L) \end{pmatrix} = \begin{pmatrix} c & s \\ c' & s' \end{pmatrix} \begin{pmatrix} x(0) \\ x'(0) \end{pmatrix}, \tag{2}$$

which is applicable for the beam transport in the absence of forces at a distance L from the grounded grid; x' is ex-

author's e-mail: emanuele.sartori@igi.cnr.it

*) This article is based on the presentation at the 26th International Toki Conference (ITC26).

pressed in radians and x in m. Using the same symbols, the Twiss parameters can also be transported:

$$\begin{pmatrix} \beta(L) \\ \alpha(L) \\ \gamma(L) \end{pmatrix} = \begin{pmatrix} c^2 & -2cs & s^2 \\ -cc' & cs' + sc' & -ss' \\ c'^2 & -2c's' & s'^2 \end{pmatrix} \begin{pmatrix} \beta(0) \\ \alpha(0) \\ \gamma(0) \end{pmatrix}. \tag{3}$$

Sticking to the definition of r_b and δ_b, and assuming beamlets are axisymmetric with respect to the beamlet axis, we can write the density in the phase space by taking into account that each i-th beamlet has a different origin coordinate (x_i, y_i). Once we assume the beamlets are cylindrical, we can use a simplified distribution for the single-beamlet density n_i in y that is a function of the beamlet width at the exit of the scanner $L + L_a$, and independent of x (see Fig. 1):

$$n_i = \frac{Ae^{-\frac{\gamma(x-x_i)^2+2\alpha(x-x_i)x'+\beta x'^2}{\varepsilon}} e^{-\frac{(y-y_i)^2}{2(r_b+(L+L_a)\delta_b)^2}}}{(r_b + (L + L_a)\,\delta_b)\,\sqrt{\pi 2}}. \tag{4}$$

3. Acceptance of the Diagnostic

The geometry of the ESS is shown in Fig. 1. In the following analytical description we will neglect the error field so that the electric field E_a along the length L_a and height H_a is uniform so that $E_a = V_a/H_a$. We will also neglect the thickness of the plates where the pinholes/slits are realized. In this case a simple parabola is used to model the particle trajectory; in the paraxial approximation the time required to travel the distance between entrance and exit apertures is $t = L_a/z'$. We can write

$$x(L + L_a) = x(L) + \theta L_a + \frac{qV_aL_a^2}{4H_aE_b}. \tag{5}$$

The entrance angles θ accepted by the exit orifice having $x_{\min} < x < x_{\max}$ vary depending on $x(L)$ and can be written

$$\begin{cases} \theta_{a\,\min}(x(L)) = \dfrac{x_{\min}}{L_a} - \dfrac{x(L)}{L_a} - \dfrac{qV_aL_a}{4H_aE_b} \\ \theta_{a\,\max}(x(L)) = \dfrac{x_{\max}}{L_a} - \dfrac{x(L)}{L_a} - \dfrac{qV_aL_a}{4H_aE_b}. \end{cases} \tag{6}$$

For a trajectory at the center of the entrance slit, the angular resolution of the diagnostic depends on the slit height $x_{\max} - x_{\min}$ and the length L_a as $\theta_{\text{res}} = (x_{\max} - x_{\min})/L_a$. Along y, the acceptance is roughly not affected by the drift inside the diagnostic if $L_a \ll L$. In terms of position, we simply have $y_{\min} < y_i(0) + (L + L_a)\cdot y'(0) < y_{\max}$, and $y_{\min,\text{entrance}} < y_i(0) + L\cdot y'(0) < y_{\max,\text{entrance}}$. In the phase space the diagnostic collects (see the acceptance shown in yellow in Fig. 2):

$$g = \sum_i \int_{x\min}^{x\max} \int_{\theta\min(x,E_a)}^{\theta\max(x,E_a)} \int_{y\min}^{y\max} \int_{-\infty}^{+\infty} n_i \mathrm{d}x\mathrm{d}x'\mathrm{d}y\mathrm{d}y'. \tag{7}$$

We have assumed that the diagnostic does not discriminate the y' space: openings are wide along y and selective to y' only at the slit edges, so that y' is integrated in $[-\infty, +\infty]$. Integral (7) is solved numerically, so that the integration intervals are calculated at different E_a, and the condition $x_{\min,\text{entrance}} < x(L) < x_{\max,\text{entrance}}$ is checked at the entrance slit.

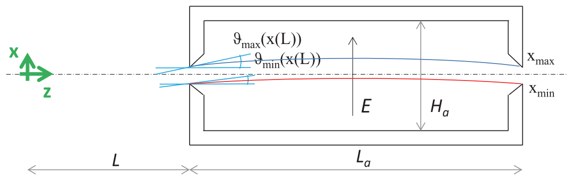

Fig. 1 ESS sketch: beam particles enter from left hand side, and a faraday cup is installed at right hand side.

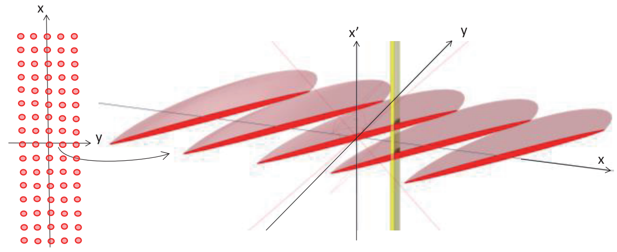

Fig. 2 Representation of: 5 beamlets on a x, y, x' projection of the phase space (red); acceptance of diagnostic (yellow).

4. Option 1 - Movable Emittance Scanner Mounted on the Movable Diagnostic Calorimeter STRIKE

The movable diagnostic calorimeter STRIKE is constituted by 16 one-dimensional CFC tiles, and it is used to map the heat flux from the beam by infrared cameras observing the rear side of the tiles. For this reason, no structures can be installed along the line of sight of the cameras. It is proposed to use a vertical, linear motion system to move the Allison scanner, and to use the same linear system to move the scanner in receded position after use. The transverse position y can be controlled by moving the STRIKE structure: the STRIKE panel is moved transversally to partially open position, in order to intercept the desired beamlet with the emittance scanner; the distance from the grounded grid can be controlled in a range between 0.6 and 1.1 m. Figure 3 exemplifies the collected signal as a function of the applied transverse electric field E_a, for different positions of the movable scanner and slit dimensions. In the calculations the beamlet temperature T_{H^-} is also varied according to $T'_{H^-}/T_{H^-} = (\omega'_c/\omega_c)^2$; note that $\omega_c = \sqrt{2}\cdot\delta_b$. The proposed setup is sketched in Fig. 4. In this configuration, the main aspect driving the design is not related to the desired performance of the diagnostic, but to the limits imposed by the heat load and by the thermal behavior of the instrument. Thermomechanical simulations were performed in order to identify

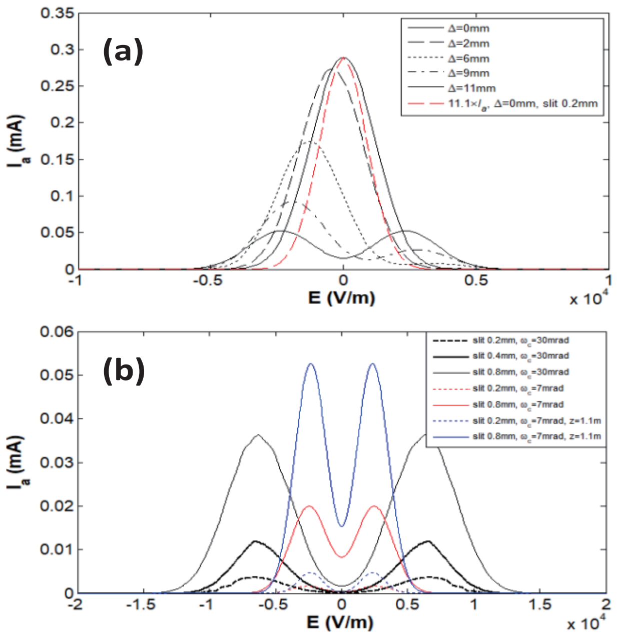

Fig. 3 Calculated signal as a function of (a) the position along x of the slit centre (ω_c = 7 mrad, z = 1.1 m, L_a = 200 mm, E_b = 22.4 keV, r_b = 5 mm, slit 0.8 mm); and of (b) the slit dimension (at a distance z = 0.6 m).

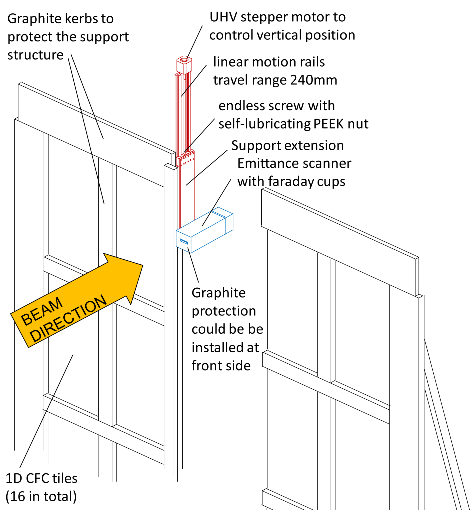

Fig. 4 Allison scanner installed on the diagnostic calorimeter.

the limits of an inertially cooled scanner (avoiding active cooling hugely simplifies the design of movable systems). The ESS structure is made of 5 mm thick stainless steel (200 × 70 × 60 mm). The footprint from nine beamlets are considered, with E_b = 22.4 keV and j = 35.5 A/m^2 providing a heat load of 800 kW/m^2. Results are shown in Fig. 5: short pulses at reduced power can be sustained by the scanner without thermal shields, which could be introduced at a second stage for high-power operations. The collected current is expected in the mA range, for a 0.2 × 30 mm slit; the residual negative ion beam fraction at z = 1 m is about 50%, due to collisional processes in the relatively high hy-

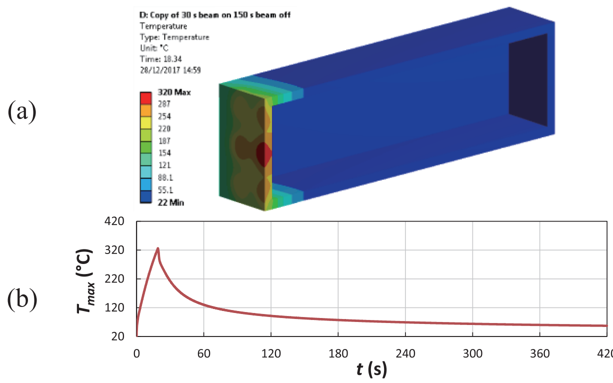

Fig. 5 Thermal simulation, whole front-surface heated: (a) temperature after 30 s, section view; (b) max temperature over time (20 s beam on, 400 s beamoff, E_b = 22.4 keV).

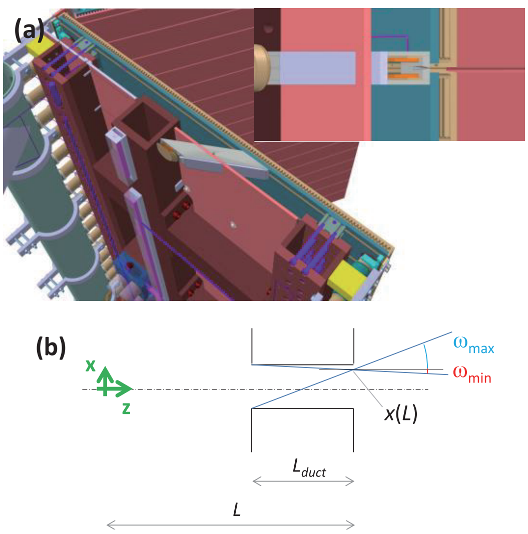

Fig. 6 (a) beam dump with fixed ESS in correspondence of the horizontal slit between behind two adjacent hypervapotron modules; (b) geometrical description of the additional slit in front of the emittance scanner.

drogen tank pressure (65 mPa [8]).

5. Option 2 - Fixed Electric-Sweep Scanner Integrated in the High-Power Beam Dump

The beam dump is composed by many independent high heat-flux water-cooled modules (hypervapotron): the modules are installed horizontally, with very thin slits between each of them. The fixed ESS can be installed in correspondence of the horizontal slit between adjacent modules, as shown in Fig. 6. If the position of the emittance scanner is fixed, only a section of the phase space can be measured; in addition, the acceptance of the scanner is affected by the slit between modules in front of the entrance slit. The elements have thickness $L_{\rm duct}$ and the height of the opening is $h_{\rm duct}$; the beam particles intercepted by a slit

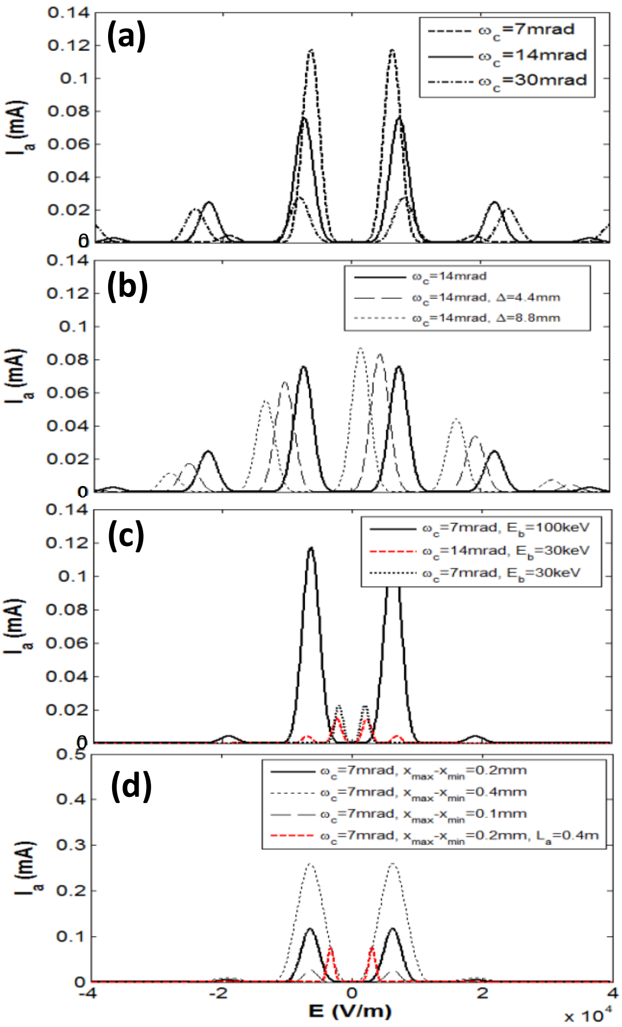

Fig. 7 Current/Electric field characteristics for different (a) beamlet optics, (b) slit positions, (c) beam energies, and (d) slit height. When not specified, $x_{\max} - x_{\min} = 0.2$ mm, $E_b = 100$ keV, $\Delta = 0$ mm, $L_a = 0.2$ m, $r_b = 5$ mm.

$x_{\min} < x < x_{\max}$, are limited in the x' space as

$$\omega_{\min} = -\arctan\left(\frac{\frac{1}{2}h_{\text{duct}} - x(L)}{L_{\text{duct}}}\right),$$
$$\omega_{\max} = \arctan\left(\frac{\frac{1}{2}h_{\text{duct}} + x(L)}{L_{\text{duct}}}\right), \quad (8)$$

where L is the position along z of the Allison scanner entrance slit. The acceptance of the slit through the beam dump elements shall give $\omega_{\min} < \theta_{\min}$ and $\omega_{\max} > \theta_{\max}$.

According to the calculation of the collected signal shown in Fig. 7 (a), the presence of the secondary peaks from neighboring beamlets gives an "intermittent" description of the angular distribution; if all beamlet optics are identical, the divergence can be obtained from the separate peaks. Figure 7 (b) shows the collected signal in the case the beamlet footprints deviate from the ideal position along x, i.e. the slit in not centered with respect to two beamlets. Basically, the figure is conceptually identical to the measurements by a movable scanner. The effect of a displacement along y is negligible for the given slit dimensions of 1cm. In the calculation we assume the beam energy and current to be at perveance match $I'_b = I_b \cdot (E'_b/E_b)^{3/2}$; the diagnostic might operate at reduced E_a, and be capable of resolving an electric current in the range of 10 μA ($E_b \sim 20$ keV) as shown in Fig. 7 (c). The slit height is proportional to the peak collected current, but it is inversely proportional to the angular resolution as shown in Fig. 7 (d). Table 1 reports example of parameters used in the calculations.

Table 1 Parameters used for the calculation.

Parameter	*values used in calculations*			
$\omega_c = \sqrt{2}\delta_b$ [mrad]	7	30	7	7
T_{H^-} [eV]	1	4	1	1
E_b [keV]	100	100	30	30
I_b [mA]	39.1	39.1	6.4	6.4
Slit height $x_{\max}-x_{\min}$ [mm]	0.2	0.2	0.2	0.4

6. Discussion

The integration of a fixed ESS in the beam dump (option 2) would allow measuring a section of the emittance in high-power scenarios, characterizing the transverse beamlet temperature and – under the assumption of identical single-beamlet optics – would provide the beam divergence. On the other hand, the proposed movable ESS (option 1) can be easily integrated in the diagnostic calorimeter STRIKE, without thermal protections in relatively-low power scenarios; it will allow the complete characterization of the single beamlet emittance along the vertical direction and it is therefore recommended. Other electric configurations for the ESS Faraday cup or additional magnetic filters may be included in the design in order to discriminate the negative ion beam fraction from the neutral beam fraction. This work was set up with partial financial support of F4E.

[1] V. Toigo *et al.*, Nucl. Fusion **57**, 086027 (2017).
[2] L.R. Grisham *et al.*, Fusion Eng. Des. **87** (11), 1805 (2012).
[3] A. Rizzolo *et al.*, Fusion Eng. Des. **123**, 768 (2017).
[4] M. Zaupa *et al.*, Rev. Sci. Instrum. **87** (11), 11D415 (2016).
[5] R. Pasqualotto *et al.*, Nucl. Instrum. Meth. A **623**, 794 (2010).
[6] P.W. Allison *et al.*, IEEE Transactions on Nuclear Science, Vol. NS-30, 2204 (1983).
[7] M. Reiser, *Theory and Design of Charged Particle Beams* (WILEY-VCH Verlag GmbH & Co, 2004).
[8] E. Sartori, G. Serianni and S. Dal Bello, Vacuum **122**, 275 (2015).